Irrigation influences on summer stream temperature variability

Abstract: Irrigation activities are a major control on water movement and storage in irrigated river valleys in the Intermountain West, USA. Particularly in dry years, surface water diversions can deplete streams over the summer irrigation season, leading to more variable stream temperatures and increased risk for resident aquatic species. Cooler lateral inflows derived from irrigation activities can mitigate the impacts of depletion by buffering main channel stream temperatures. Given the increasing susceptibility of depleted streams to climate and land use changes, understanding stream temperature patterns and controls in these systems is critical. We used intensive field monitoring over three summers and thermal aerial imagery to characterize stream temperature patterns and irrigation influences in a 2.5 km reach of a small agricultural stream in northern Utah. Considering variable hydrology, weather, channel morphology, diversions, and lateral inflows we found stream temperatures to be relatively insensitive to flow depletion or lateral inflows in a wet year but very sensitive in drier years. Irrigation-related lateral inflows reduced longitudinal warming and diel variability during drier years and at times prevented temperatures from reaching stressful or lethal limits. Reaches with substantial lateral inflow contributions also had a greater areal proportion of low temperatures and spatial temperature diversity. These trends were enhanced by differences in channel morphology, with greater spatial and temporal variability in multi-thread than single-thread reaches. Study results highlight critical flow and weather conditions driving increased temperature variability that will likely become more extreme with additional climate change related reductions in baseflow. Regardless of the cause, this study highlights that decreased instream flows increase the importance of identifying, quantifying, and maintaining lateral inflows to maintain instream temperatures and preservation of these inflows should be considered in future water management decisions.

Key words: stream temperature; irrigation; surface fluxes; lateral inflows; thermal imagery; thermal refugia; aquatic ecosystems; summer baseflow

Introduction

Irrigated agriculture is the dominant water use in the western U.S., accounting for more than 90% of surface water demands (Maupin et al., 2014). Peak irrigation demands generally occur during the dry season from June to September when plant water demands are high and streamflow is naturally lowest. Historically, irrigators in the region have had little to no restriction on the amount of water left in-stream (Szeptycki, Forgie, Hook, Lorick, & Womble, 2015). Combined with mounting climate and population stressors (Fritze, Stewart, & Pebesma, 2011; Mankin & Diffenbaugh, 2014), surface water diversions and groundwater pumping for irrigation are driving more frequent and intense streamflow depletion over the dry season. Streamflow depletion is defined here as any human-driven reduction in flow below unimpaired conditions ranging from minor reductions in flow to full channel dewatering. Past research has provided strong evidence that agricultural management practices influence baseflows (Condon & Maxwell, 2014; Ferguson & Maxwell, 2011; Kendy & Bredehoeft, 2006), but research that specifically links diversions and other irrigation activities to stream temperature responses is limited (Essaid & Caldwell, 2017).

Under depleted low flow conditions, stream temperatures are much more susceptible to heating and increased variability due to increased surface area to water volume ratios and

dominant solar radiation influences (Bingham, Neilson, Neale, & Cardenas, 2012; Neilson, Stevens, Chapra, & Bandaragoda, 2009). Channel morphology can also influence the surface area available for exchanges at the air-water interface (Brown, 1969; Brown & Krygier, 1970; Poole & Berman, 2001; Schmadel, Neilson, & Heavilin, 2015; Sinokrot & Stefan, 1993; Stonedahl, Harvey, & Packman, 2013), potentially exacerbating this low flow sensitivity when channels are very wide and flow depth is shallow. Given ongoing and planned stream channel modifications in the Intermountain West, such as for flood conveyance (i.e., riprap, weirs, dredging, and channelization), it is also critical to understand the impacts of changes in morphology on stream temperature in depleted stream reaches.

Lateral inflow contributions to stream channels, which can consist of deep groundwater, shallow subsurface flow, or overland flow, can mitigate the impacts of depletion by supplementing main channel flow (Buahin, Horsburgh, & Neilson, 2019; King, Neilson, Overbeck, & Kane, 2016; Wetstein & Hasfurther, 1989). Previous studies have shown up to 80% of dry season baseflows have been attributed to lateral inflows in irrigated basins (Kahlown & Kemper, 2004). Subsurface flow contributions can buffer stream temperatures in the main channel during low flow conditions (Buahin et al., 2019; Tague & Grant, 2009), reduce the rate of temperature increase and even decrease main channel stream temperature (Dzara, Neilson, & Null, 2019; Poole & Berman, 2001), providing critical thermal refugia for aquatic species (Isaak et al., 2018; Miller, Wooster, & Li, 2007). Despite mounting interest in the role of lateral inflows in depleted streams, these contributions have proven difficult to quantify given that they are highly variable in space and time (Schmadel, Neilson, & Kasahara, 2014). Furthermore, their influence on main channel temperature depends on other factors. The temperature and volume of lateral inflows, which may vary with season and water management, can dictate their overall importance and whether they warm or cool the stream, making it necessary to directly identify and monitor these inflows in sensitive systems (Buahin et al., 2019; Dzara et al., 2019; Essaid & Caldwell, 2017; Garner, Malcolm, Sadler, & Hannah, 2014; Kahlown & Kemper, 2004; King et al., 2016; Linstead, 2018; Luce et al., 2014; Mayer, 2012).

Given the dominance of irrigated agriculture in the Intermountain West and the increasing susceptibility of depleted streams to temperature variability under climate and land use changes, understanding of the linkages between flow depletion, irrigation-related lateral inflows, and summer stream temperatures is critical. This study aims to characterize these linkages in a typical irrigated intermountain valley stream by evaluating the influences of lateral inflows on stream temperature in the context of variable hydrology, weather, and channel morphology. We do this by characterizing longitudinal stream flow and temperature patterns in a depleted study reach influenced by adjacent irrigation and unlined distribution canals over three consecutive summers. We analyze these data in the context of thermal tolerance thresholds for resident aquatic species. The resulting relationships are expected to reflect broader hydrologic trends across irrigated western river valleys and provide foundational information to guide water and natural resource management in these systems.

Study Area

The Blacksmith Fork River (BSFR) begins in the mountains of northern Utah and drains a 743 km^2 watershed into an agricultural river valley before merging with the Bear River which terminates in the Great Salt Lake. It has an average elevation of 2,150 meters above sea level, average annual flow of 3.05 cubic meters per second (cms) and average annual precipitation of 73 cm. Similar to many streams in the Intermountain West, the BSFR receives much of its water from snowpack occurring at mid-elevation locations (<3,000 m), making it particularly sensitive

to changes in climate, with peak flows in spring and naturally low flows during the summer and fall (Jain & Lall, 2000; Serreze, Clark, Armstrong, McGinnis, & Pulwarty, 1999). Below the canyon mouth, the BSFR is diverted six times for irrigation over 13 km before reaching the confluence with the Logan River (Figure 1a).

[Figure 1]

A 2.5 km section in the BSFR valley from Nibley BSF Main Canal to the Millville Providence BSF Lower Canal (Figure 1a) was selected as the study reach for its established seasonal flow depletion due to three upstream agricultural diversions. Several diversions feed 3 unlined earthen canals that parallel the study reach on both sides. All of these canals flow at higher elevations than the river, creating large head gradients towards the river. Lateral inflows, defined here as seeps or other subsurface flow contributions originating from flood irrigation, canal seepage, and/or deep groundwater sources, have been observed to provide flow to both the river and irrigation canals. For example, groundwater seeps and springs, a number of which are used as drinking water sources, occur along the terrace west of the study area. These provide additional flow to nearby canals and a local source of shallow groundwater recharge. Flow depletion through the study reach can result in exposed banks, isolated pools, channel separation, and even full channel dewatering in very dry years (Figure 1c). During these very dry years, local landowners provided qualitative information about river sections that would maintain pools or even continue to have flowing water, suggesting general locations for lateral inflows to the river.

The study reach also includes a mixture of multi-thread and single-thread channel morphology. Multi-thread reaches occur in unconfined settings with multiple flow paths, small side channels and deep pools, while single thread reaches have relatively uniform channels and many have been channelized or modified for better flood conveyance (Figure 1b and 1c). An electrofishing survey in the study reach by the Utah Division of Wildlife Resources in 2019 and conversations with adjacent landowners suggest that the reach supports a substantial brown and rainbow trout population (>100 fish per mile) when flow and temperature conditions are sufficient. Due to mounting impacts of diversions on local river ecosystems and fishing opportunities, there is growing interest among basin stakeholders to better balance irrigation demands with flow and temperature requirements for these aquatic species during the water-limited summer period (Lane & Rosenberg, 2020).

Methods

Study Design

The study reach (Figure 1a) was segmented into six reaches (R1-R6) ranging from 367 to 472 meters in length to isolate the influences of channel morphology and lateral inflow sources while maintaining relatively even spacing between measurements, as constrained by river access (Figure 2). Four of these reaches (R2-R5) with distinct channel morphology were classified as either single- or multi-threaded based on field observations and aerial imagery for subsequent analyses. Six distinct lateral inflow locations, primarily in the form of seeps, were identified through field observation, stream temperature and water quality monitoring, and analysis of thermal imagery as described below.

[Figure 2]

Data Collection

To address the research objectives, discharge and stream temperature data were collected along the study reach over summers 2018 (May to August), 2019 (June to November), and 2020 (June to September) (Figure 2). We installed one vented CS450 pressure transducer (Campbell Scientific, Logan UT) upstream of the Nibley BSF Main Canal and one unvented Level TROLL 400 pressure transducer (In-Situ, Fort Collins CO) in the Nibley BSF Main Canal (Figure 2) to measure water depth at 15-minute intervals. A BaroTroll pressure transducer (In-Situ, Fort Collins CO) was also installed near the canal to correct for atmospheric pressure. Depth was converted to discharge using rating curves that relate water surface elevation to streamflow measurements at the two locations (*SI* Figure 1). 15-minute solar radiation and air temperature data were obtained from a nearby Logan River Observatory weather station (Logan River Observatory, 2020).

Daily streamflow just below the Nibley BSF Main Canal diversion [river meter (RM) 0] was obtained using a flow balance approach, where the downstream flow was estimated as the measured flow above Nibley BSF Main Canal minus the measured flow in the canal. Point discharge measurements at all three locations were used to validate this flow balance to ensure there were no unaccounted gains or losses between flow measurement locations. To augment discharge estimates obtained from the gauging stations, synoptic point discharge measurements were taken over a 1-2 day timeframe at five locations in 2018 and seven locations in 2019 and 2020 using a FlowTracker (SonTek, San Diego CA) (Figure 2) to provide information regarding reach scale gains and losses during different flow conditions. Discharge measurements in 2019 occurred later in the summer due to limited accessibility during the higher early summer flow.

Two methods were used to collect stream temperature data along the study reach. Sixteen HOBO Pro V2 stream temperature sensors (Onset, Bourne, MA) were installed along the main channel of the study reach (Figure 2) to collect stream temperature data at 15-min intervals. Thermal imagery was also collected for the entire study reach on August 25, 2018, providing high-resolution gridded raster data of stream temperature under depleted late summer conditions. A fixed wing unmanned aerial vehicle from the AggieAir UAV Program (Utah State University, Logan UT) was flown 350 m above the ground with two scientific grade optical sensors, capturing narrowband red, green, blue and near infrared information (6.7 cm resolution), and one radiometrically calibrated temperature sensor (42 cm resolution). Images were captured at 1 Hz cadence. Aerial imagery was calibrated to the installed temperature sensors described above as well as eight additional sensors strategically placed instream for the duration of the flight to capture the full range of temperature exhibited over the study reach (Jensen, Neilson, McKee, & Chen, 2012).

The locations of substantial lateral inflow contributions were identified in the field in 2018 and validated with spot stream temperature measurements indicating cool and constant temperature signatures relative to the main channel. Stream temperature sensors were installed in each identified lateral inflow in 2019 and 2020 (Figure 2). Only LI-3,4,5 had sufficient flow to be instrumented in 2020. Each sensor was fully submerged in the lateral inflow above the confluence with the main channel.

To better understand sources of lateral inflows, water quality measurements were made in the main channel at the beginning and end of the study reach, in a downstream section of the canal that represents a mix of river water and deep groundwater springs, in the two large springs, and in LI-1 through LI-6 (Figure 2) on 8/6/2019. Specific conductivity measurements were taken with a 6920 Multi-Parameter Water Quality Sonde (YSI, Yellow Spring OH). Grab samples were collected and analyzed for anions (chloride, sulfate, nitrate) and cations (sodium, calcium, magnesium). Samples were filtered with a 0.45 um nylon filter into acid-washed LDPE bottles. Anion samples were frozen and cation samples were acidified with nitric acid and refrigerated. Samples were analyzed by ion chromatography using a Dionex DX-1300 ion chromatograph.

Data Analysis

Hydrologic variability

Daily flow depletion in the study reach was estimated to provide insight regarding the portion of water removed from the stream over time. Daily depletion was calculated as the difference between unimpaired streamflow at the USGS gaging station (10113500) in Blacksmith Fork canyon upstream from the study reach (RM -9600) and the estimated streamflow below the Nibley BSF Main Canal (RM 0). This measure accounts for any inflows between these locations as well as the three major diversions above RM 0 (Millville Providence Upper Canal, Hyrum Canal, and Nibley BSF Main Canal) (Figure 1a, Figure 2).

To assess hydrologic conditions over the study period relative to the long-term interannual climate variability, water year types were determined from the upstream unimpaired USGS streamflow gage record based on available data from 1913-2019 (with data missing from 9/30/1996 - 3/21/2000). Average summer baseflow in each water year was calculated as the average daily streamflow from June 1 to September 31 to correspond with the irrigation season. Each water year was assigned as wet (>75th percentile), moderate (25-75th percentile), or dry (<25th percentile) based on its ranked average summer baseflow.

Lateral inflows

Temperature differences between sensors in main channel and nearby lateral inflows were assessed by plotting 15-min stream temperature time series over all summers. Although lateral inflows were not instrumented in 2018, a sensor placed at RM 2014 was later found to be capturing lateral inflow contributions and monitored in later years as LI-5. Temperature at this sensor was plotted against the main channel temperature at RM 1851 downstream to compare lateral inflow temperatures between years.

Synoptic stream flow and temperature analysis

Stream channel flow differencing was performed to identify gaining and losing reaches along the study reach and evaluate how those trends vary seasonally and interannually. Each reach was characterized as gaining (%ΔQn>0), losing (%ΔQn<0), or no change (%ΔQn=0) based on:

$$\%\Delta Q_n = \left[\frac{Q_d - Q_u}{L_n \times Q_u} \right] \times 100$$

where %ΔQn is the percent change in flow based on the difference between downstream (Q_d) and upstream (Q_u) measurements over reach n, normalized by reach length $L_n$and upstream flow

Q_u. Gaining reaches indicate the presence of lateral inflow sources by assuming hyporheic gains or losses have flow path lengths shorter than the sub-reaches.

A similar analysis was performed to evaluate longitudinal warming and cooling trends through time as the percent change in temperature over reach *n*, normalized by reach length and upstream temperature ($\%\Delta T_n$). Each reach (R1-R6) was evaluated based on differences between upstream and downstream measurements to determine if it was warming ($\%\Delta T_n>0$), cooling ($\%\Delta T_n<0$), or no change ($\%\Delta T_n=0$). The temperature sensors located nearest each of the discharge measurement locations were used to calculate change within a reach, based on average hourly stream temperature at 16:00 hr to represent a warm time of day (R packages *ggplot2*, *dplyr*, *reshape2*).

Longitudinal stream temperature trends

Several analyses were performed to explore the relationship between weather, flow, and stream temperature. Space-time plots (R package *oce*) were generated with 15-minute stream temperature data to visualize variability along the study reach and through time. Observed differences in diel variability on warm versus cool days in 2018 prompted an additional assessment of daily maximum, minimum, and average stream temperatures at each main channel sensor along the study reach on days with very different average daily air temperature.

The thermal imagery was evaluated with respect to the reaches defined above (Figure 2) using spatial statistics in an effort to isolate the influences of channel morphology and lateral inflows on spatial stream temperature patterns. ArcGIS (ESRI, 2017) was used to clip thermal and near-infrared imagery to the RBG imagery of the river corridor. A normalized difference vegetation index (NDVI) layer was generated from the near-infrared imagery to identify a threshold of 0.2 to separate areas without (>0.2) and with (<0.2) vegetation. Next, a temperature threshold was used to distinguish water (<28 °C) from dry land (>28 °C) in the thermal imagery. Since some vegetation was captured using this threshold due to evapotranspiration, the NDVI and thermal layers were combined to clip the channel boundary. The clipped thermal imagery was evaluated with respect to channel reach morphology by comparing single-thread (R2, R4) and multi-thread (R3) reaches, and with respect to lateral inflow contributions by comparing multi-thread reaches without (R3) and with (R5) field-identified lateral inflows. Finally, time series and distributions of hourly longitudinal stream temperature change (ΔT/km) over classified reaches R2-R5 were used to explore differences in the frequency and magnitude of heating and cooling between reaches and years.

Results

Interannual hydrologic variability

Average summer streamflow at the USGS gaging station varies substantially from year to year. Drier conditions have become more frequent through time, with only two of the 26 wet years over the 106-year period of record (8%) occurring in the past 33 years. All three years of data collection were classified as moderate water years, although average unimpaired summer streamflow was 3.93 cms in 2019 but only 2.43 cms in 2018 and 2.52 cms in 2020. Both unimpaired and depleted daily flows were substantially lower in 2018 and 2020 than 2019 (Figure 3a). Diversion rates and associated flow depletion increased over the summer, with maximum depletion occurring on July 13 in 2018 at 72%, July 24 in 2019 at 47%, and August 20

in 2020 at 73% and eventually returning to unimpaired conditions at the end of the irrigation season in October (Figure 3b).

[Figure 3]

Notably, although 2018 and 2020 had similar unimpaired and depleted streamflow patterns (Figure 3a), depletion patterns were distinct (Figure 3b), with greater depletion generally occurring when solar radiation and air temperature are higher (Figure 3c) - presumably due to increased water demands for irrigation. Specifically, diversions began earlier in 2018, with flow at RM 0 depleted to 1 cms by mid-June 2018 while flow did not drop below 1 cms until mid-July in 2020 (Figure 3b). In August and September there were periods of lower air temperature that did not correspond to reduced diversions. The large reduction in depletion in September 2020 corresponded with a major wind storm that forced diversions to be closed due to debris in the channel.

Six major lateral inflow contributions were identified along the study reach (Figure 2) through a combination of visual inspection, temperature sampling, and thermal imagery. The lateral inflows generally had very consistent temperatures through time and across years while the nearby main channel temperature exhibited greater diel and interannual variability. For example, temperature patterns in LI-5 were quite consistent between 2018 and 2019 (Figure 4). All stream temperature plots are available in Supplemental Information (*SI* Figure 2). Across all years and locations monitored, lateral inflows had average temperatures of 11.2 – 12.3 ^{0}C and variance ranging from 0.5 ^{0}C at LI-4 to 6.05 ^{0}C at LI-2. All lateral inflows shifted from being cooler than the main channel to warmer than the main channel at some point between late July and early September as solar radiation influences diminished during the fall and winter periods.

[Figure 4]

Specific conductance of lateral inflows LI-1 through LI-5 was relatively consistent across measurement locations (457-474 µS/cm, Figure 5). These values are similar to RM 0 and RM 2500 that had 421 and 430 uS/cm, respectively. The smallest, most downstream inflow (LI-6) had higher values (556 uS/cm), and the deep groundwater springs had substantially higher values (810 and 933 µS/cm). Similarly, other ion concentrations show that while LI-1 through LI-5 are chemically similar to the river and the canal concentrations, LI-6 and the deep groundwater springs have notably higher concentrations of chloride, nitrate, sodium, potassium, and magnesium (Figure 5). These results combined with the large head gradients between the canals and the river suggest that LI-1 through LI-5 were likely derived from shallow subsurface seepage from irrigation related recharge or nearby unlined canals (e.g., Hyrum BSF Canal and/or Nibley BSF Canal) paralleling the main channel. The origin of LI-6 may also be a canal (e.g., Millville Providence BSF Upper Canal that runs at a much higher elevation along the bench) or nearby irrigation, however, the chemical signature of this inflow is more similar to that of deep groundwater.

[Figure 5]

Synoptic flow and temperature study

Synoptic flow and temperature measurements (Table 1) revealed clear longitudinal trends over each summer and year (Figure 6). Across years, warming trends generally corresponded with losing or neutral reaches and cooling trends with gaining reaches during the irrigation season, but these trends are reversed in late summer when the main channel becomes cooler than lateral inflows (Figure 4). R5 consistently gains the largest percentage of flow during summer (i.e., all monitoring dates except November 2019) with as much as 80% gains under the lowest measured flow conditions (July 20 2018, 0.38 cms), corresponding with identified lateral inflow contributions. R3 generally loses the most flow, with up to 29% in mid-summer, although it is a gaining reach in June 2018.

[Table 1] [Figure 6]

In the highest summer flow conditions of 2019, longitudinal and seasonal temperature trends were evident but muted (Figure 6). On July 22 and August 29 of 2019, warming occurred in R1-R4 and R6. R5 – the reach where the most substantial lateral inflows occur – shifted from slight cooling to substantial warming over the three measurement dates. By November 8, R1, R2, R4, and R6 were still warming, but R3 shifted to slight cooling. Maximum warming (8% in R4) occurred in November and maximum cooling (-2% in R5) occurred in July. This is consistent with results from the previous analysis indicating that the main channel is warmer than lateral inflows and therefore susceptible to cooling until mid-August to early September, at which point lateral inflows actually warm the stream.

Observed longitudinal trends in 2018 and 2020 were generally similar but more pronounced than those in 2019, with much larger within-reach changes in flow and temperature. In 2018, longitudinal temperature change trends in R1 to R5 were generally consistent over the summer. Note that 2018 discharges were averaged over R1-R2 and over R3-R4 because discharge measurements were collected at fewer locations. R1-R4 warmed, R5 cooled substantially, and R6 shifted from slight warming to slight cooling. This within-reach warming was most extreme on July 20, 2018 under 71% depletion, with 19% warming in R4 and -17% cooling in R5 corresponding with lateral inflows. Compared to 2019, maximum percent warming and cooling were increased by 11% and -14%, respectively, in 2018. Notably, the percent of flow gained in R5 was far greater in July 2018 than July 2019, resulting in over five times more cooling. August 2020 trends were similar to those of July 2018 in R1-R4, reflecting similar streamflow patterns (Figure 3a). However, in the most downstream reach, gains and cooling trends in R5 were maintained through R6 in July 2018, while R6 had returned to a warming reach by August 2020.

Longitudinal trends in stream temperature

Space-time plots illustrate 15-minute stream temperature variability along the study reach in July, the month with greatest solar radiation influences (Figure 7). In all three years, stream temperatures increase from RM 0 to RM 1851, at which point temperatures peak and then decrease. These trends are most pronounced in 2018, followed by 2020. 2019 exhibits substantially less diel variability and downstream warming, with a daily maximum stream temperature of 17 °C at RM 1851, 4.7 °C cooler than the 2018 maximum. However, longitudinal warming and diel variability also vary substantially between days within each summer, due primarily to variability in local weather conditions (Figure 3c and d).

[Figure 7]

Longitudinal trends are most pronounced in July 2018 and to a lesser extent in August 2020 (Figure 7). On July 10, 2018, when 15-minute stream temperatures reached their maximum and air temperature was high (26.2 °C), the most upstream sensor (RM 0) ranged 3.3 °C (14.5 to 17.9 °C) and this diel range increased downstream to a maximum of 6.5 °C (15.2 to 21.7 °C) at RM 1851 (Figure 7b). A sharp decrease in maximum temperature was recorded in R5 between RM 1851 and RM 2060 where lateral inflows were observed, and then cooling continued to the downstream end of the study reach. By contrast, a week earlier when average daily air temperature was only 17.3 ^{0}C, the maximum diel stream temperature range at RM 1851 was only 1.9 ^{0}C (12.7 to 14.6 ^{0}C), with the most upstream and downstream sensors exhibiting ranges <2 ^{0}C (Figure 7a).

Longitudinal stream temperature patterns are also influenced by channel reach morphology. The thermal imagery collected August 25, 2018 shows distinct temperature distributions between single- and multi-thread reaches and reaches without or with lateral inflows (Figure 8). Between the multi-thread reaches, median temperatures were cooler and the interquartile range larger in the upstream reach without lateral inflows (R3: 16.5 ^{0}C, 15.2 to 23.3 ^{0}C) than the downstream reach with lateral inflows (R5: 17.2 ^{0}C, 16.3 to 21.9 ^{0}C) (Figure 8a). Among the three reaches with minimal lateral inflow contributions, multi-thread R3 had a slightly higher median temperature and interquartile range compared to R2 (15.9 ^{0}C, 15.0 to 21.5 ^{0}C) and R4 (16.1 ^{0}C, 15.4 to 21.0 ^{0}C). This finding contrasts with the longitudinal warming generally observed from R2 to R4 in the 15-minute temperature series, particularly under low flows (Figure 6 and 7).

[Figure 8]

Time series of hourly longitudinal stream temperature change show differences in frequency and magnitude of heating between reaches. Multi-thread R3 heats more during the day and cools more at night than single-thread R2 (Figure 9). It also spends less time warming over the summer, with fewer time intervals where $\Delta T/km>0$ in R3 than R2 (Figure 9 a-c) as exhibited by distributions being shifted to the left (*SI* Figure 3). The frequent cooling exhibited by R3 may also explain why R4, located directly downstream, had a slightly lower median temperature on the date of aerial imagery collection even though the spatial distribution is skewed towards warmer temperatures (Figure 8). By contrast, single-thread R4 is always warming over the summer and exhibits greater diel variability in warming rates than upstream reaches (>3.5 ^{0}C/km) (Figure 9 d-f). Lateral inflow contributions in R5 result in cooling during the entire irrigation season in all years, although the magnitude of cooling varies by season and year, with the most cooling in mid-summer 2018 under depleted low flow conditions (<-4 ^{0}C/km). Additionally, the portion of the summer that R4 spends warming and R5 spends cooling increases substantially in drier years, while these interannual differences are less apparent between R2 and R3 (Figure 9; *SI* Figure 3).

[Figure 9]

Discussion

Dominant physical controls on stream temperature patterns have been studied for decades, and it is well established that human activities can affect stream temperature through changes in the timing and magnitude of thermal energy delivered to the channel (heat load) or the amount of water in the channel (flow regime) (e.g., Brown & Krygier, 1970; Webb & Zhang, 1997). However, the specific influences of irrigation activities on the flow regime and heat load of western streams remain poorly understood (Poole & Berman, 2001). This research gap is likely due in part to the local influences of diversions and lateral inflows in irrigated systems, which are variable in space and time and have proven difficult to quantify. Our study used intensive field monitoring over three summers to quantify stream temperature patterns in a small intermountain agricultural stream in the context of variable hydrology, weather, channel morphology, and lateral inflow contributions.

As expected, stream temperatures were most sensitive to heat exchanges under low flows and high depletion - including surface heat fluxes (radiative, sensible, latent heat exchanges) and lateral inflows. The moderate summers of 2018 and 2020 exhibited more pronounced stream temperature variability and daily maximum temperatures in response to surface heat fluxes and lateral inflows than the wet summer of 2019 (Figures 3, 6, 7, 9). While summers 2018 and 2020 had very similar unimpaired streamflow patterns, slowly receding from 3 to 2 cms from mid-June to October (Figure 3a), distinct weather conditions and associated diversion activities resulted in distinct stream temperature responses (Figure 3b and c). Greater depletion generally corresponded with higher air temperatures due to increased water demands for irrigation. However, periods of lower solar radiation and air temperature did not always correspond with reduced diversions, likely due to water management practices whereby diversions are increased to meet increased water demands but not necessarily reduced as demands drop. In moderate years, stream temperatures were most sensitive to diversions when high air temperatures correspond with high solar radiation. Enhanced warming effects observed in July 2018 compared to August 2020 despite similar flows and air temperatures suggest that, under sufficiently low flow conditions, stream temperature variability most directly reflects differences in seasonal air temperature patterns in the absence of lateral inflows.

Despite capturing substantial hydrologic variability, our study does not reflect the full range of natural interannual variability exhibited by this or other mid-elevation western streams. Recorded average summer streamflows over the century at the Blacksmith Fork USGS gage were as much as 68% lower than what was monitored from 2018 to 2020 (Figure 3a). Furthermore, mounting climate change impacts in mid-elevation western streams will likely exacerbate the stream temperature trends observed in the two moderate flow years. Mid-elevation snowmelt-dominated watersheds are particularly sensitive to climate changes (Barnett, Adam, & Lettenmaier, 2005; Jain & Lall, 2000; Serreze et al., 1999). The compounding effects of reduced snowpack, increased melt rate, higher air temperatures, and increased agricultural water demands will likely lead to more frequent and longer lasting critical conditions than were observed in this study (Barnett et al., 2005; Elias et al., 2016). Additional monitoring over hotter and drier years is needed to characterize these responses.

Surface heat fluxes

Under low flow conditions, BSFR stream temperatures became increasingly sensitive to atmospheric exchanges with higher diversion rates. Irrigation diversions upstream from the study reach reduced unimpaired flow by up to 70% (Figure 3), reducing water depth and velocity which translates to higher surface area to volume ratios and longer residence times (Johnston & Naiman, 1987). Longer residence times mean more energy exchange can occur across the air–water interface and these small parcels of slower moving water are more susceptible to external influences (e.g., Gu, Montgomery, & Austin, 1998; Majerova, Neilson, & Roper, 2020). Upstream from lateral inflow contributions (R1-R4), increasing depletion from 55 to 70% corresponded with more downstream warming and diel temperature variability (Figures 3, 6, 7, 9). These observed trends are caused by solar energy gains during the day and energy losses at night due primarily to longwave radiation exchange. In a similar depleted stream, Meier, Bonjour, Wüest, and Reichert (2003) simulated a similar magnitude of warming driven primarily by solar radiation heat exchanges using a physically-based temperature model. These warming patterns also correspond with previous research on differential heating in reaches with distinct surface area to volume ratios, although in our study the increased surface area to volume ratio is due to water withdrawals in addition to differences in channel setting (Allanson & Gieskes, 1961; Clark, Webb, & Ladle, 1999; Majerova et al., 2020). With sufficient streamflow, such as during the higher flow summer of 2019, diel variability is dampened and stream temperatures remain relatively stable regardless of weather conditions (Figure 7, Figure 9). It should be noted that bed sediment heat fluxes (hyporheic exchange, bed conduction) and the localized influence of riparian shading were not considered here. Given the reach widths and channel orientation, shading influences are greater both early and late in the day, but should not alter the maximum temperatures significantly over the study reach. Based on modeling studies conducted in the nearby Logan River, hyporheic exchange could, however, potentially influence within-day temperature variability (Buahin et al., 2019).

Temperature responses to diversions in the BSFR were generally consistent with other seasonally depleted western streams. For instance, a stream temperature model simulating different water diversion scenarios in another Intermountain stream found that diversions in July and August increase average daily maximum temperatures by 2.0 °C in a wet year and 3.3 °C in a dry year (Dzara et al., 2019). In another seasonally depleted stream in northern California, simulated diversions caused a ~2 °C increase in average summer stream temperature (Liu et al., 2017). Similar to our study, the highest diversion rates and depletion levels were associated with the most extreme stream temperature increases. Liu et al. (2017) also found that streams with naturally high baseflow contributions are less susceptible to extreme temperature variability. The natural baseflow contributions discussed in their study appear to serve a similar buffering role to irrigation-sourced lateral inflows in the BSFR.

Channel morphology influences enhanced by diversions

Channel reach morphology, and specifically whether a reach is single-threaded or more complex multi-threaded, appears to influence stream temperature patterns in space and time, and differences are more pronounced under low flows and during the irrigation season (Figure 8). Similar to past studies (Harvey & Bencala, 1993; Hawkins, Hogue, Decker, & Feminella, 1997; Poole & Berman, 2001), the multi-thread reach (R3) in the BSFR generally heats more during the day and cools more at night than upstream single-thread R2 (Figure 9). R3 also experiences

net warming for less time over the summer than R2 or R4 (Figure 9, *SI* Figure 3). Similar to the influence of depletion, the increased diel variability associated with complex multi-thread channels is likely attributable to the larger surface area to water volume ratios and longer residence times (Brown, 1969; Brown & Krygier, 1970; Gu et al., 1998; Johnston & Naiman, 1987; Sinokrot & Stefan, 1993). However, contrary to these trends, single-thread R4 exhibits greater diel variability than upstream multi-thread R3 in drier years (Figure 9). In fact, R4, which likely has the smallest surface area to volume ratio, exhibits the highest relative longitudinal warming of any reach (Figure 6) and warms consistently over all summers (Figure 6, Figure 9). This may be explained by high flow losses in R3 (up to 30%) (Figure 6), which cause R4 to have the lowest ambient streamflow of any reach. Therefore, while multi-thread reaches have the potential to warm more during the day than single-thread reaches under depleted conditions (and similar flow levels), they also have the potential to cool more, have portions that are shaded, and exhibit more diverse temperature conditions.

Lateral inflows dampen temperature variability under depleted conditions

Lateral inflow contributions along the downstream portion of the study reach buffer the system under highly depleted low flow conditions, reducing both longitudinal warming and diel variability. During the warm low flow season, lateral inflows were cooler relative to the main channel and these temperature differences became more pronounced under increasing depletion (Figure 4). Particularly in drier years, lateral inflows reduced within-reach warming and even shifted the main channel to a cooling state, while similar contributions had an almost undetectable influence in 2019 (Figure 6, Figure 7). This is similar to previous findings that temporal patterns in gaining reaches due to groundwater inflows consistently exhibit negative correlations between streamflow and both stream temperature and temperature variability (e.g., Constantz, 1998; Silliman & Booth, 1993). However, before and after the irrigation season, lateral inflows were warmer relative to the main channel due to higher flows and cooler air temperatures (Figure 4). Essaid and Caldwell (2017) observed similar seasonal trends in another irrigated western river valley. The thermal imagery reveals the localized thermal refugia and increased spatial stream temperature diversity occurring at lateral inflow locations (Figure 8). Highlighting the importance of this hydrologic pathway, some researchers have proposed actively generating points of focused lateral inflows as a viable mechanism by which to create thermal refugia (Kurylyk, MacQuarrie, Linnansaari, Cunjak, & Curry, 2015).

While our study does not explicitly quantify the portion of diverted flow that returned to the stream via subsurface flow paths, stream flow and temperature observations (Figure 6) combined with the specific conductance and ion concentrations (Figure 5) indicate that in the two moderate summers, a significant portion of flow in R5 and R6 is most likely attributable to lateral inflows sourced from unlined earthen canals and irrigation activities in adjacent fields that parallel the river. The specific conductance and ion concentrations of identified lateral inflows (except LI-6) were indistinguishable from the adjacent canals and main channel and very different from nearby groundwater springs (Figure 5). A study of a similar Intermountain valley stream in Montana found that surface water irrigation under current practices (primarily flood and sprinkler irrigation) resulted in substantial subsurface lateral inflows that made up 60-70% of flow in late summer (Essaid & Caldwell, 2017). Based on a coupled surface water-groundwater model, lateral inflows resulted in 0.7 °C/km of downstream cooling, and shifting from surface to groundwater irrigation substantially reduced late summer streamflow and cooling trends.

Lateral inflows have an ecologically relevant influence on stream temperature

Stream temperature directly influences aquatic species metabolic rates, physiology, and life-history traits and affects rates of important community processes such as nutrient cycling and productivity (Brown, Hannah, & Milner, 2004; Gasith & Resh, 1999). Stream temperature fluctuations caused by variable meteorological factors and human activities can therefore substantially impact the stress and survival of aquatic species (Webb, Hannah, Moore, Brown, & Nobilis, 2008; Yearsley, 2009). Irrigation-depleted reaches in particular often occur in critical aquatic migratory corridors between steep mountain canyons and high-order floodplains and historically hosted higher levels of biodiversity than colder headwater streams (Isaak et al., 2018), making elevated stream temperatures even more consequential. Results from our study suggest that, under high solar radiation and air temperature conditions, flow diversions can shift streams into thermally stressful conditions for resident aquatic species, even in moderate years (Figure 10). At the same time, applied irrigation water can infiltrate into the subsurface, cooling as it moves through the ground, and return to the stream as lateral inflows resulting in downstream cooling (Essaid & Caldwell, 2017) or via seepage in unlined canals. Significant lateral inflows in the study reach reduced longitudinal warming and diel variability and at times prevented temperatures from reaching stressful or lethal limits. For instance, on warm days in 2018, maximum daily stream temperatures were reduced from above the stress limit (>19 °C) down to the growth range for brown trout just downstream from lateral inflows (RM 1850) (Figure 10b). Highlighting the importance of lateral inflows for maintaining suitable habitat conditions in the BSFR, temperature observations upstream from lateral inflows in the study reach correspond with previous studies that have linked temperature effects of irrigation diversions with severe consequences for aquatic species (Bauer et al., 2015; Bunn & Arthington, 2002; Dewson, James, & Death, 2007; Miller et al., 2007).

[Figure 10]

Water management implications

In light of increasing competition over diminishing and increasingly unpredictable water resources, western natural resource managers face a mounting challenge to more efficiently allocate water to both instream and extractive demands. Several policy tools are available to address this challenge, including implementing water efficiency measures (e.g., lining and piping canals), water rights transfers, and regulatory water temperature standards (Elmore, Null, & Mouzon, 2016; Grafton et al., 2018; Olden & Naiman, 2010). Effective use of these policy tools requires explicit consideration of their effects on stream temperature under different hydrologic, weather and morphological conditions. Results from this study highlight critical conditions for extreme warming and stream temperature variability during which reducing diversions or transferring agricultural or municipal water rights to instream could sustain sensitive aquatic species.

This study also provides a basis for quantifying possible effects of irrigation efficiency measures on summer stream temperature and associated habitat for aquatic species. Lining or piping earthen canals and switching from flood to sprinkler irrigation are being used to reduce losses as water becomes scarcer and more expensive (Grafton et al., 2018). These measures reduce the amount of irrigation water that returns to streams via the subsurface as cooler lateral inflows.

Specifically, we identified lateral inflow locations and characterized patterns of flow gains and losses and associated temperature changes under variable hydrology and weather. The compounding effects of climate change and reduced lateral inflows are likely to increase summer temperature variability and peak daily temperature in western agricultural streams. Additional research is needed to further quantify the separate and combined influences of flow depletion and lateral inflows in irrigated basins across a range of geologic and soil settings, canal network topologies, and irrigation practices. Future research using statistical and physically-based modeling could provide a deeper understanding of the controls on stream temperature and effects of specific climate or management changes.

Conclusions

This study characterized summer stream temperature patterns and irrigation influences in a typical small snowmelt-fed western agricultural stream. Using three summers of intensive field monitoring and thermal aerial imagery, we demonstrate the interacting influences of hydrology, weather, channel morphology, and irrigation activities on stream temperature patterns and highlight the critical role of lateral inflows. Interannual hydrologic variability was a dominant control on temperature response to depletion, with relatively stable stream temperatures in a wet summer and substantial diel variability and longitudinal temperature change in years with moderate streamflow. In moderate years, irrigation diversions increased surface area to volume ratios which increased downstream daily maximum temperatures. These trends were enhanced by differences in channel morphology, with greater temporal variability and spatial diversity in multi-thread than single-thread reaches and less time spent warming over the summer. Irrigation-related lateral inflows were shown to provide important thermal resets under depleted low flow conditions, reducing downstream warming and diel variability and at times preventing temperatures from reaching thermal tolerance limits for resident aquatic species. Field observations and statistical analyses highlighted critical flow and solar radiation conditions during which diversion limits or instream water transfers could sustain temperature-sensitive aquatic species. Regional climate changes including reduced baseflow and increased air temperature are expected to have cascading hydrologic effects and result in higher demands for less water, increasing competition between extractive and instream water needs. Under these conditions, stream temperatures in western snowmelt-fed agricultural streams will become even more sensitive to irrigation activities, and lateral inflows will likely play an increasingly important role as a thermal buffer. Climate and land use changes will further necessitate monitoring to characterize effects on the timing, magnitude and temperature of lateral inflows and associated stream temperature patterns.

Data Availability Statement

Data and code are available in the Hydroshare database: Alger, M. and Lane, B. (2020). Irrigation influences on summer stream temperature variability, HydroShare. DOI Pending

Citations

Allanson, Brian R, and J Gieskes. 1961. 'Investigations into the ecology of polluted inland waters in the Transvaal', *Hydrobiologia*, 18: 2-2.

Barnett, T. P., J. C. Adam, and D. P. Lettenmaier. 2005. 'Potential impacts of a warming climate on water availability in snow-dominated regions', *Nature*, 438: 303-9.

Bauer, Scott, Jennifer Olson, Adam Cockrill, Michael Van Hattem, Linda Miller, Margaret Tauzer, and Gordon Leppig. 2015. 'Impacts of surface water diversions for marijuana cultivation on aquatic habitat in four northwestern California watersheds', *PLoS One*, 10: e0120016.

Bingham, QG, Bethany T Neilson, CMU Neale, and MB Cardenas. 2012. 'Application of high−resolution, remotely sensed data for transient storage modeling parameter estimation', *Water Resources Research*, 48.

Brown, George W. 1969. 'Predicting Temperatures of Small Streams', *Water Resources Research*, 5: 68-75.

Brown, George W., and James T. Krygier. 1970. 'Effects of Clear-Cutting on Stream Temperature', *Water Resources Research*, 6: 1133-39.

Brown, Lee. E, David M. Hannah, and Alexander M. Milner. 2004. 'Alpine Stream Temperature Variability and Potential Implications for Benthic Communities', *Hydrology: Science & Practice for the 21st Century*, 2.

Buahin, Caleb A, Jeffery S Horsburgh, and Bethany T Neilson. 2019. 'Parallel multi-objective calibration of a component-based river temperature model', *Environmental Modeling & Software*, 116: 57-71.

Bunn, Stuart E., and Angela H. Arthington. 2002. 'Basic Principles and Ecological Consequences of Altered Flow Regimes for Aquatic Biodiversity', *Environmental Management*, 30: 492-507.

Clark, E, BW Webb, and M Ladle. 1999. 'Microthermal gradients and ecological implications in Dorset rivers', *Hydrological Processes*, 13: 423-38.

Condon, Laura E., and Reed M. Maxwell. 2014. 'Groundwater-fed irrigation impacts spatially distributed temporal scaling behavior of the natural system: a spatio-temporal framework for understanding water management impacts', *Environmental Research Letters*, 9: 034009.

Constantz, Jim. 1998. 'Interaction between stream temperature, streamflow, and groundwater exchanges in alpine streams', *Water Resources Research*, 34: 1609-15.

Dewson, Zoë S., Alexander B. W. James, and Russell G. Death. 2007. 'A review of the consequences of decreased flow for instream habitat and macroinvertebrates', *Journal North American Benthological Society*, 26: 401-15.

Dzara, Jessica R, Bethany T Neilson, and Sarah E Null. 2019. 'Quantifying thermal refugia connectivity by combining temperature modeling, distributed temperature sensing, and thermal infrared imaging', *Hydrology and Earth System Sciences*, 23: 2965.

Elias, Emile, Al Rango, Ryann Smith, Connie Maxwell, Caiti Steele, and Kris Havstad. 2016. 'Climate Change, Agriculture and Water Resources in the Southwestern United States', *Journal of Contemporary Water Research & Education*, 158: 46-61.

Elmore, L. R., S. E. Null, and N. R. Mouzon. 2016. 'Effects of Environmental Water Transfers on Stream Temperatures', *River Research and Applications*, 32: 1415-27.

Essaid, H. I., and R. R. Caldwell. 2017. 'Evaluating the impact of irrigation on surface water - groundwater interaction and stream temperature in an agricultural watershed', *Sci Total Environ*, 599-600: 581-96.
Ferguson, Ian M., and Reed M. Maxwell. 2011. 'Hydrologic and land–energy feedbacks of agricultural water management practices', *Environmental Research Letters*, 6: 014006.
Fritze, Holger, Iris T. Stewart, and Edzer Pebesma. 2011. 'Shifts in Western North American Snowmelt Runoff Regimes for the Recent Warm Decades', *Journal of Hydrometeorology*, 12: 989-1006.
Garner, Grace, Iain A Malcolm, Jonathan P Sadler, and David M Hannah. 2014. 'What causes cooling water temperature gradients in a forested stream reach?', *Hydrology and Earth System Sciences*, 18: 5361.
Gasith, Avital, and Vincent H. Resh. 1999. 'Streams in Mediteranean Climate Regions: Abiotic Influences and Biotic Responses to Predictable Seasonal Events'.
Grafton, RQ, John Williams, CJ Perry, Francois Molle, Claudia Ringler, Pasquale Steduto, Brad Udall, SA Wheeler, Yahua Wang, and Dustin Garrick. 2018. 'The paradox of irrigation efficiency', *Science*, 361: 748-50.
Gu, Ruochuan, Shawn Montgomery, and T Al Austin. 1998. 'Quantifying the effects of stream discharge on summer river temperature', *Hydrological Sciences Journal*, 43: 885-904.
Harvey, Judson W., and Kenneth E. Bencala. 1993. 'The Effect of streambed topography on surface-subsurface water exchange in mountain catchments', *Water Resources Research*, 29: 89-98.
Hawkins, Charles P., James N. Hogue, Lynn M. Decker, and Jack W. Feminella. 1997. 'Channel Morphology, Water Temperature, and Assemblage Structure of Stream Insects', *Journal of the North American Benthological Society*, 16: 728-49.
Isaak, Daniel J, Charles H Luce, Dona L Horan, Gwynne L Chandler, Sherry P Wollrab, and David E Nagel. 2018. 'Global warming of salmon and trout rivers in the Northwestern US: road to ruin or path through purgatory?', *Transactions of the American Fisheries Society*, 147: 566-87.
Jain, Shaleen, and Upmanu Lall. 2000. 'Magnitude and timing of annual maximum floods: Trends and large-scale climatic associations for the Blacksmith Fork River, Utah', *Water Resources Research*, 36: 3641-51.
Jensen, Austin M, Bethany T Neilson, Mac McKee, and YangQuan Chen. 2012. "Thermal remote sensing with an autonomous unmanned aerial remote sensing platform for surface stream temperatures." In *2012 IEEE International Geoscience and Remote Sensing Symposium*, 5049-52.
Johnston, Carol A, and Robert J Naiman. 1987. 'Boundary dynamics at the aquatic-terrestrial interface: the influence of beaver and geomorphology', *Landscape Ecology*, 1: 47-57.
Kahlown, M. A., and W. D. Kemper. 2004. 'Seepage losses as affected by condition and composition of channel banks', *Agricultural Water Management*, 65: 145-53.
Kendy, Eloise, and John D. Bredehoeft. 2006. 'Transient effects of groundwater pumping and surface-water-irrigation returns on streamflow', *Water Resources Research*, 42.
King, Tyler V, Bethany T Neilson, Levi D Overbeck, and Douglas L Kane. 2016. 'Water temperature controls in low arctic rivers', *Water Resources Research*, 52: 4358-76.
Kurylyk, Barret L, Kerry TB MacQuarrie, Tommi Linnansaari, Richard A Cunjak, and R Allen Curry. 2015. 'Preserving, augmenting, and creating cold−water thermal refugia in rivers:

Concepts derived from research on the Miramichi River, New Brunswick (Canada)', *Ecohydrology*, 8: 1095-108.
Lane, Belize A., and David E. Rosenberg. 2020. 'Promoting In-Stream Flows in the Changing Western US', *Journal of Water Resources Planning and Management*, 146: 02519003.
Linstead, Conor. 2018. 'The Contribution of Improvements in Irrigation Efficiency to Environmental Flows', *Frontiers in Environmental Science*, 6.
Liu, Dedi, Y. Xu, S. Guo, L. Xiong, P. Liu, and Q. Zhao. 2017. 'Stream temperature response to climate change and water diversion activities', *Stochastic Environmental Research and Risk Assessment*, 32: 1397-413.
Logan River Observatory (2020). Logan River Observatory: Logan River Golf Course Climate Site (LR_GC_C) Quality Controlled Data, HydroShare, http://www.hydroshare.org/resource/86a27290e1b443a488f0b84cb9e2af91.
Luce, Charles, Brian Staab, Marc Kramer, Seth Wenger, Dan Isaak, and Callie McConnell. 2014. 'Sensitivity of summer stream temperatures to climate variability in the Pacific Northwest', *Water Resources Research*, 50: 3428-43.
Majerova, Milada, Bethany T Neilson, and Brett B Roper. 2020. 'Beaver dam influences on streamflow hydraulic properties and thermal regimes', *Science of the Total Environment*, 718: 134853.
Mankin, Justin S., and Noah S. Diffenbaugh. 2014. 'Influence of temperature and precipitation variability on near-term snow trends', *Climate Dynamics*, 45: 1099-116.
Maupin, Molly A. , Joan F. Kenny, Susan S. Hutson, John K. Lovelace, Nancy L. Barber, and Kristin S. Linsey. 2014. 'Estimated Use of Water in the United States in 2010'.
Mayer, Timothy D. 2012. 'Controls of summer stream temperature in the Pacific Northwest', *Journal of Hydrology*, 475: 323-35.
Meier, Werner, Cyrill Bonjour, Alfred Wüest, and Peter Reichert. 2003. 'Modeling the effect of water diversion on the temperature of mountain streams', *Journal of Environmental Engineering*, 129: 755-64.
Miller, Scott W, David Wooster, and Judith Li. 2007. 'Resistance and resilience of macroinvertebrates to irrigation water withdrawals', *Freshwater Biology*, 52: 2494-510.
Neilson, B. T., D. K. Stevens, S. C. Chapra, and C. Bandaragoda. 2009. 'Data collection methodology for dynamic temperature model testing and corroboration', *Hydrological Processes*, 23: 2902-14.
Olden, Julian D., and Robert J. Naiman. 2010. 'Incorporating thermal regimes into environmental flows assessments: modifying dam operations to restore freshwater ecosystem integrity', *Freshwater Biology*, 55: 86-107.
Poole, Geoffery C, and Cara H Berman. 2001. 'Pathways of human influence on water temperature dynamics in stream channels', *Environmental Management*, 27: 787-802.
Schmadel, Noah M, Bethany T Neilson, and Justin E Heavilin. 2015. 'Spatial considerations of stream hydraulics in reach scale temperature modeling', *Water Resources Research*, 51: 5566-81.
Schmadel, Noah M, Bethany T Neilson, and Tamao Kasahara. 2014. 'Deducing the spatial variability of exchange within a longitudinal channel water balance', *Hydrological Processes*, 28: 3088-103.
Serreze, Mark C., Martyn P. Clark, Richard L. Armstrong, David A. McGinnis, and Roger S. Pulwarty. 1999. 'Characteristics of the western United States snowpack from snowpack telemetry (SNOTEL) data', *Water Resources Research*, 35: 2145-60.

Silliman, Stephen E, and David F Booth. 1993. 'Analysis of time-series measurements of sediment temperature for identification of gaining vs. losing portions of Juday Creek, Indiana', *Journal of Hydrology*, 146: 131-48.
Sinokrot, Bashar A., and Heinz G. Stefan. 1993. 'Stream temperature dynamics: Measurements and modeling', *Water Resources Research*, 29: 2299-312.
Stonedahl, Susa H., Judson W. Harvey, and Aaron I. Packman. 2013. 'Interactions between hyporheic flow produced by stream meanders, bars, and dunes', *Water Resources Research*, 49: 5450-61.
Szeptycki, Leon F. , Julia Forgie, Elizabeth Hook, Kori Lorick, and Philip Womble. 2015. 'Environmental Water Rights Transfers: A Review of State Laws'.
Tague, Christina, and Gordon E. Grant. 2009. 'Groundwater dynamics mediate low-flow response to global warming in snow-dominated alpine regions', *Water Resources Research*, 45.
Webb, Bruce W, David M Hannah, R Dan Moore, Lee E Brown, and Franz Nobilis. 2008. 'Recent advances in stream and river temperature research', *Hydrological Processes*, 22: 902-18.
Webb, BW, and Y Zhang. 1997. 'Spatial and seasonal variability in the components of the river heat budget', *Hydrological Processes*, 11: 79-101.
Wetstein, J H, and Victor R. Hasfurther. 1989. 'Irrigation Diversion and Return Flows - Pinedale', *Wyoming Water Developement Commission*.
Yearsley, John R. 2009. 'A semi−Lagrangian water temperature model for advection−dominated river systems', *Water Resources Research*, 45.

Tables

Table 1. Synoptic discharge measurement dates and measured discharge at RM 0.

Date	Discharge (cms)
6/15/2018	1.23
6/25/2018	0.72
7/20/2018	0.38
7/22/2019	1.80
8/29/2019	1.37
11/8/2019	2.61
8/19/2020	0.45

Figure Legends

Figure 1. (a) The study reach (red) of the Blacksmith Fork River (blue) in northern Utah, with 4 of the 6 major diversions (red arrows), adjacent canals (teal), and lateral inflows (blue arrows) indicated. Images of study reach under (b) natural summer low flow conditions and (c) depleted and fully dewatered conditions.

Figure 2. Study site schematic including six reaches (R1-R6), canals, and locations of pressure transducers, synoptic discharge measurements, two large deep groundwater springs, stream temperature sensors, and lateral inflows (LI). Only LI-5 was monitored in all three years. Two discharge locations were only monitored in 2019 and 2020. Flow is from top to bottom.

Figure 3. (a) Average daily unimpaired streamflow at the USGS gaging station and depleted streamflow at the upstream end of the study reach (0 m) in summers 2018 - 2020. (b) Percent depletion relative to unimpaired flow. Average daily solar radiation, air temperature, and stream temperature at RM 1851 in moderate years (c) 2018 and (d) 2020.

Figure 4. Hourly temperature plots of the main channel at RM 1851 and lateral inflow LI-5 in 2018 and 2019 show consistent lateral inflow temperatures between years.

Figure 5. Specific conductivity and ion samples on 8/6/2019 from lateral inflows (LI), Nibley BSF Canal (NBSF), RM0, RM2500, and deep groundwater springs (S) shown in Figure 2.

Figure 6. Synoptic flow and stream temperature trends over the study duration, including measurement date and discharge at RM 0. Lateral inflows in R5 increase relative change in flow ($\%\Delta Q$) and reduce relative warming ($\%\Delta T$) in all years. Combined bars in 2018 for reaches R1-R2 and R3-R4 are due to fewer discharge measurement locations in this year.

Figure 7. Space-time plots of 15-minute stream temperature for July 2018, 2019, and 2020, where flow is from bottom to top of panel and study reaches R1-R6 are indicated. Temperatures generally increase longitudinally until RM 1851, where lateral inflows act as a thermal reset.

Figure 8. (a) Spatial stream temperature distributions and (b) thermal imagery on the date of aerial imagery collection in reaches R2-R5. Flow is from right to left.

Figure 9. Plots of hourly longitudinal stream temperature change in four reaches (R2 - R5) over summers 2018-2020 over the monitoring periods, where $\Delta T/km>0$ indicates warming. R3 and R5 have multi-thread channel morphology, and the majority of lateral inflows occur in R5.

Figure 10. Space-time stream temperature plot for July 2018 with insets of daily stream temperature range (min, mean, and max) on (a) a cool day (average air temp 17.7 °C) and (b) a warm day (26.2 °C). Major lateral inflows are indicated by blue arrows. Each point represents a temperature sensor along the main channel, and stressful (19 °C) and lethal (24.5 °C) brown trout thermal tolerances are indicated.

Supplemental Information

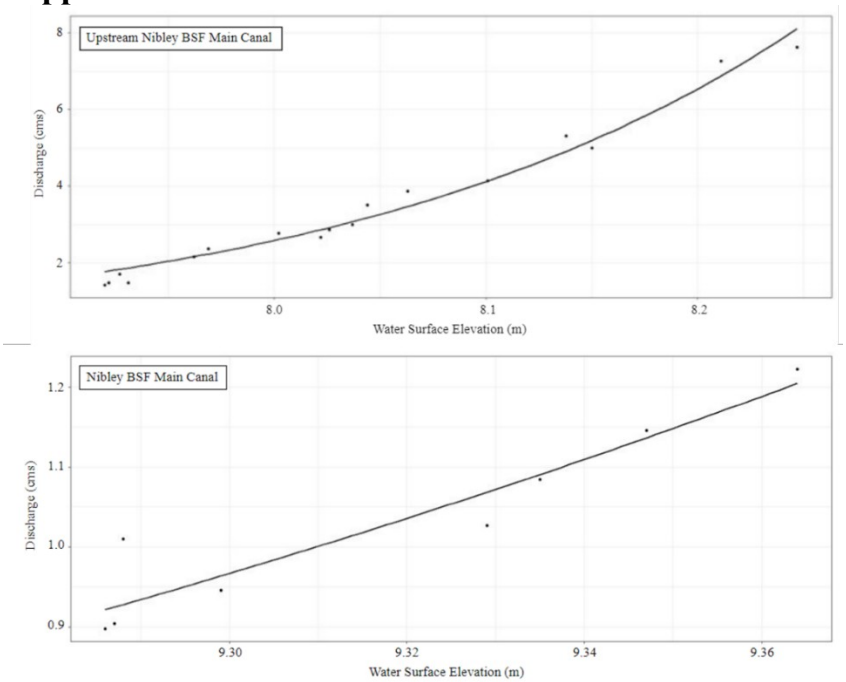

Figure 1. Water surface elevation – streamflow rating curves (a) BSFR above Nibley BSF Canal and (b) in Nibley BSF Canal

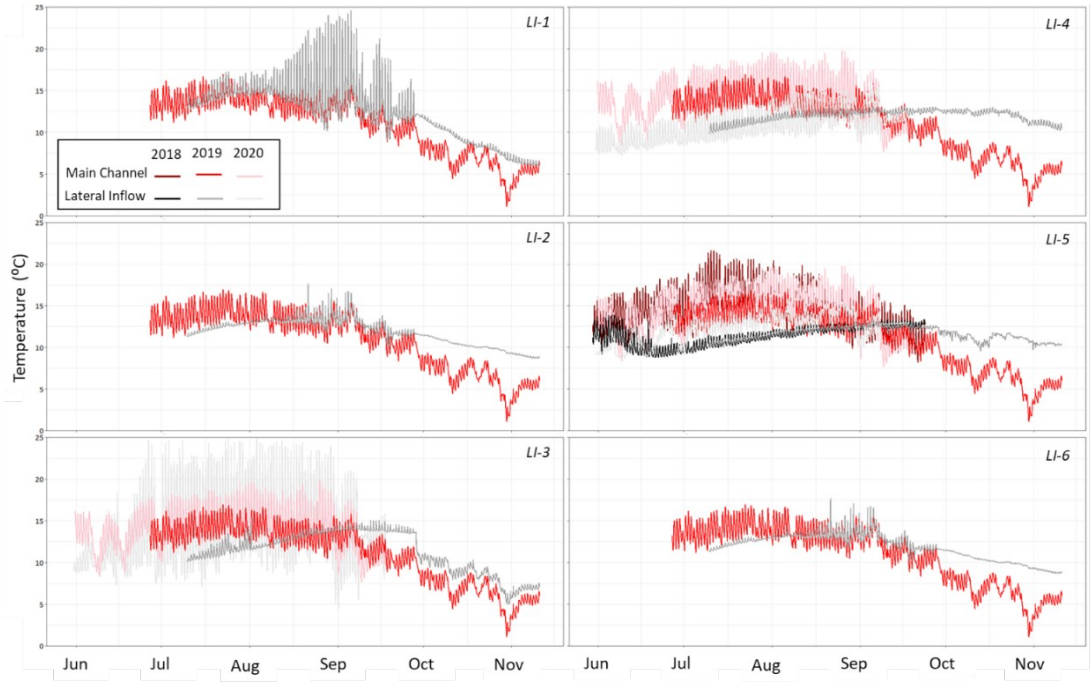

Figure 2. Hourly temperature plots of lateral inflows and the nearest main channel sensor for all monitored locations and years. High diel variability in LI temperatures may indicate LI sensors are in the mixing zone or exposed to air, as seen in LI-1 in 2019 and LI-3 in 2020.

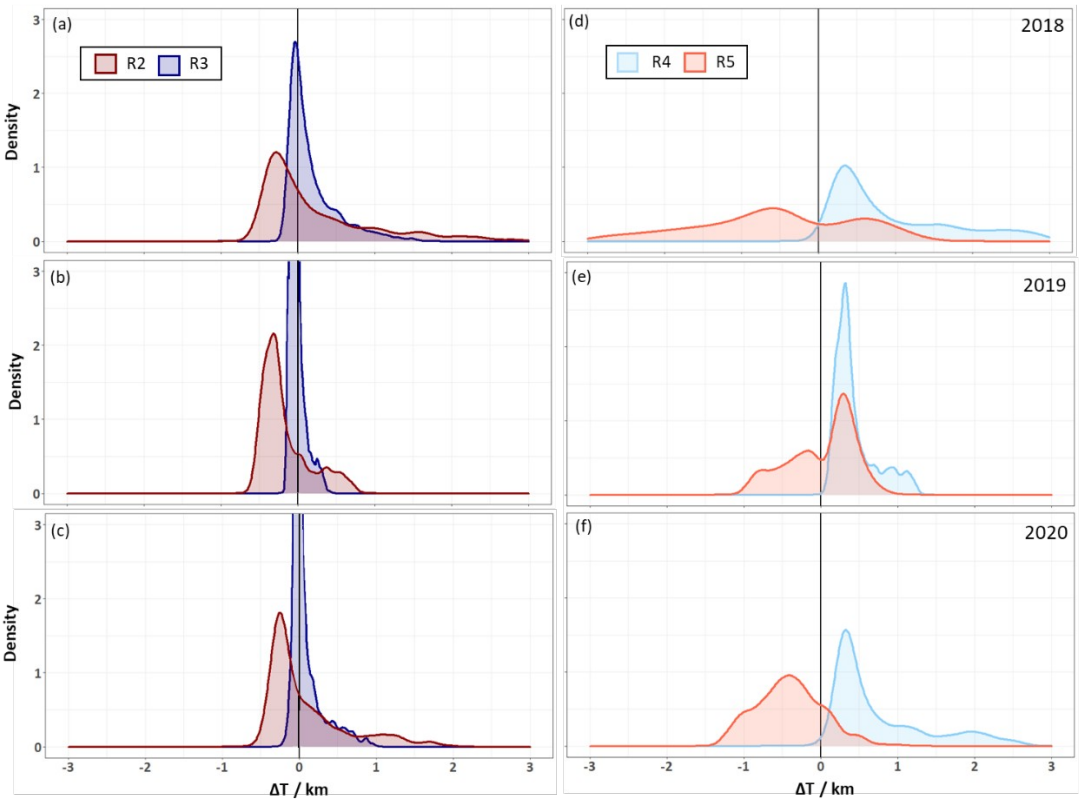

Figure 3. Distribution of hourly longitudinal stream temperature change in four stream reaches (R2-R5) over three summer monitoring period, where $\Delta T/km>0$ indicates warming.